



Molecular basis of conjugation-mediated DNA transfer by gram-negative bacteria

Gabriel Waksman^{1,2}

Bacterial conjugation is the unidirectional transfer of DNA (often plasmids, but also other mobile genetic elements, or even entire genomes), from a donor cell to a recipient cell. In Gram-negative bacteria, it requires the formation of three complexes in the donor cell: i-a large, double-membrane-embedded transport machinery called the Type IV Secretion System (T4SS), ii-a long extracellular tube, the conjugative pilus, and iii-a DNA-processing machinery termed the relaxosome. While knowledge has expanded regarding molecular events in the donor cell, very little is known about the machinery involved in DNA transfer into the recipient cell. Here, focusing on systems principally involved in DNA transfer, we provide an update on progress made on various mechanistic aspects of conjugation.

Addresses

¹ Institute of Structural and Molecular Biology, School of Natural Sciences, Birkbeck College, Malet Street, London, WC1E 7HX, United Kingdom

² Institute of Structural and Molecular Biology, Division of Biosciences, University College London, Gower Street, WC1E 6BT, United Kingdom

Corresponding author: Waksman, Gabriel (g.waksman@bbk.ac.uk), (g.waksman@ucl.ac.uk)

Current Opinion in Structural Biology 2025, 90:102978

This review comes from a themed issue on **Macromolecular Assemblies (2025)**

Edited by **Chris Hill** and **Elena Orlova**

For a complete overview see the [Issue](#) and the [Editorial](#)

Available online xxx

<https://doi.org/10.1016/j.sbi.2024.102978>

0959-440X/© 2024 The Author. Published by Elsevier Ltd. This is an open access article under the CC BY license (<http://creativecommons.org/licenses/by/4.0/>).

Keywords

Type IV Secretion Systems, T4SS, Relaxosome, Conjugative pilus, Bacterial conjugation, DNA transfer.

Introduction

Bacterial conjugation, discovered by Lederberg and Tatum in 1945, is a process by which DNA, generally plasmids or other mobile genetic elements, but also genomes, are transported unidirectionally from a donor cell that contains the plasmid to a recipient cell that does not [1]. Conjugation plays crucial roles in horizontal gene

transfer and therefore bacterial evolution and adaptation, and more particularly constitutes the principal means by which antibiotic resistance genes spread among some of the most dangerous pathogen populations [2–4].

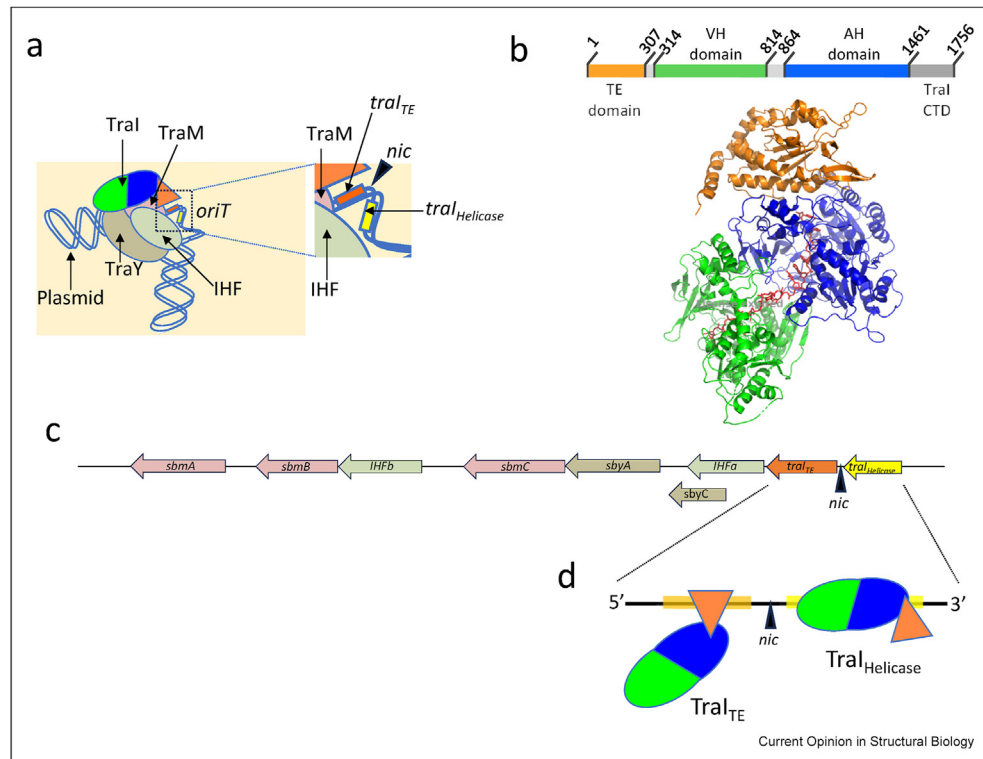
While very little is known regarding the molecular requirements in the recipient cell, knowledge about the molecular events taking place in the donor cell has expanded rapidly. In the donor cell, the formation and action of three complexes are required: a DNA-processing machinery, called “relaxosome,” that primes the DNA before transport, a transport machinery, called the Type IV Secretion System (T4SS), that powers the DNA through the bacterial double-membrane, and a long tubular helical polymer, the pilus, through which the DNA might pass to reach the recipient cell [5–9]. While the T4SS is responsible for DNA transport, it is also responsible for pilus biogenesis. Thus, the T4SS plays two fundamental roles: first it must elaborate a pilus, and once this task is completed, it must switch to DNA transfer. We focus here on the structurally much better-known complexes of Gram-negative bacteria.

The relaxosome

The relaxosome is a large complex that acts as a DNA processing machinery. The relaxosome’s primary roles are i- to prime the DNA for subsequent transfer and ii-together with the T4SS ATPase VirD4, and using the helicase unwinding activity of one of its components, to power the transfer of DNA through the T4SS, through the pilus, into the recipient cell [10,11].

Here, we will describe the relaxosome encoded by F-family plasmids, one of the best studied complexes of its kind. In F, the relaxosome is composed of 4 proteins assembling in various stoichiometries (Figure 1a). The largest and most essential component is TraI, the so-called relaxase (1756 residues) [12]. It forms a complex with three accessory proteins, TraY (131 residues) [13], IHF (a heterodimer of IHF α and IHF β , (99 and 94 residues, respectively)) [14] and TraM (a homotetramer of 127 residues subunits) [15], at a defined site on the F plasmid called *oriT* (Figure 1a). The TraI relaxase is a bi-functional enzyme that contains 4 domains: a trans-esterase (TE) domain that displays a nicking and joining activity, two helicase domains (one vestigial (VH), so called because it has lost its

Figure 1



The relaxosome, the Tral relaxase, and the *oriT* region. **a**) Schematic diagram of the relaxosome. The assembled relaxosome structure is not known and therefore, only a diagram is shown. All proteins are labeled, as is *oriT*, where only the two Tral binding sites, *tral_{TE}* (in orange) and *tral_{Helicase}* (in yellow) are shown. The three main domains of Tral are colored as in **b**. In the zoom-in on *oriT*, the *nic* site is shown. **b**) Structure of the "tight" protease resistant form of Tral (Tral_{Helicase}) bound to ssDNA via its helicase domains. Representation is in orange, green, and blue ribbon for the TE, VH, and AH domains, respectively. ssDNA is in red stick representation. A schematic representation of the domain structure of Tral is shown above the structure. Boundary residues for each domain are indicated. **c**) The entire *oriT* region of the F plasmid. The *oriT* region contains two Tral binding sites (*tral_{TE}* in orange and *tral_{Helicase}* in yellow), 2 IHF $\alpha\beta$ binding sites (*IHF α* and *IHF β*), 2 x TraY binding sites (*sbyA* and *sbyC*), and 3 TraM binding sites (*sbmA-C*). Color coding of the IHF, TraY, TraM binding site is as in **a** for each individual protein. **d**) Zoom in on the Tral binding sites with two Tral proteins bound, one (Tral in its "loose/flexible" conformation (Tral_{TE})) bound to the DNA sequence in orange (representing the *tral_{TE}* binding site 5' of *nic*) through its TE domain, and the other (Tral in its "tight" conformation (Tral_{Helicase})) bound to the DNA sequence in yellow (representing the *tral_{Helicase}* binding site 3' of *nic*) through its helicase VH and AH domains.

unwinding catalytic residues, and one active (AH)), and a C-terminal domain (CTD), which may interact with TraM [15,16] (Figure 1b). *oriT* is about 400 base pairs in size and contains two binding sites for TraI, two for TraY, two for IHF, and three for TraM (Figure 1c) [17–19]. The two binding sites of TraI are located on each side of an important site termed the "nic" site (Figure 1, a and c) [16]. This site is located on the strand of DNA that is destined for transfer, the T-strand. During DNA processing, the T-strand is nicked at *nic*, and the relaxase reacts covalently with the 5' phosphate resulting from the nicking reaction. Thus the substrate to be transferred is actually a protein-ssDNA conjugate. TraI exists in two conformations, open and closed, also termed TraI_{TE} and TraI_{Helicase}, respectively, depending on where TraI binds [16] (Figure 1d). Indeed, when bound to the sequence 3' of *nic* (in yellow, site called *tral_{Helicase}* in Figure 1, a, c and d), TraI is in a closed

compact form and binds ssDNA through its helicase domains, hence its name TraI_{Helicase}. Its structure has been determined by cryo-EM (Figure 1b) [16]. In contrast, when bound to the sequence 5' of *nic* (in orange, site called *tral_{TE}*, in Figure 1, a, c and d), it is in an open conformation and bound through its TE domain (hence its name TraI_{TE}) [16]. The TraI_{TE} structure is unknown. Remarkably, the two TraI binding sites were shown to accommodate two TraI molecules simultaneously, one bound 3' of *nic* in the closed TraI_{Helicase} conformation, the other bound 5' of *nic* in the open TraI_{TE} conformation (Figure 1d) [16].

At some point during conjugation (see details below), the relaxosome is recruited to the T4SS via interactions of TraM with the C-terminal tail of VirD4 [20]. It may also occur through interactions of subdomains of TraI VH and AH with yet-to-be-identified T4SS partners [21].

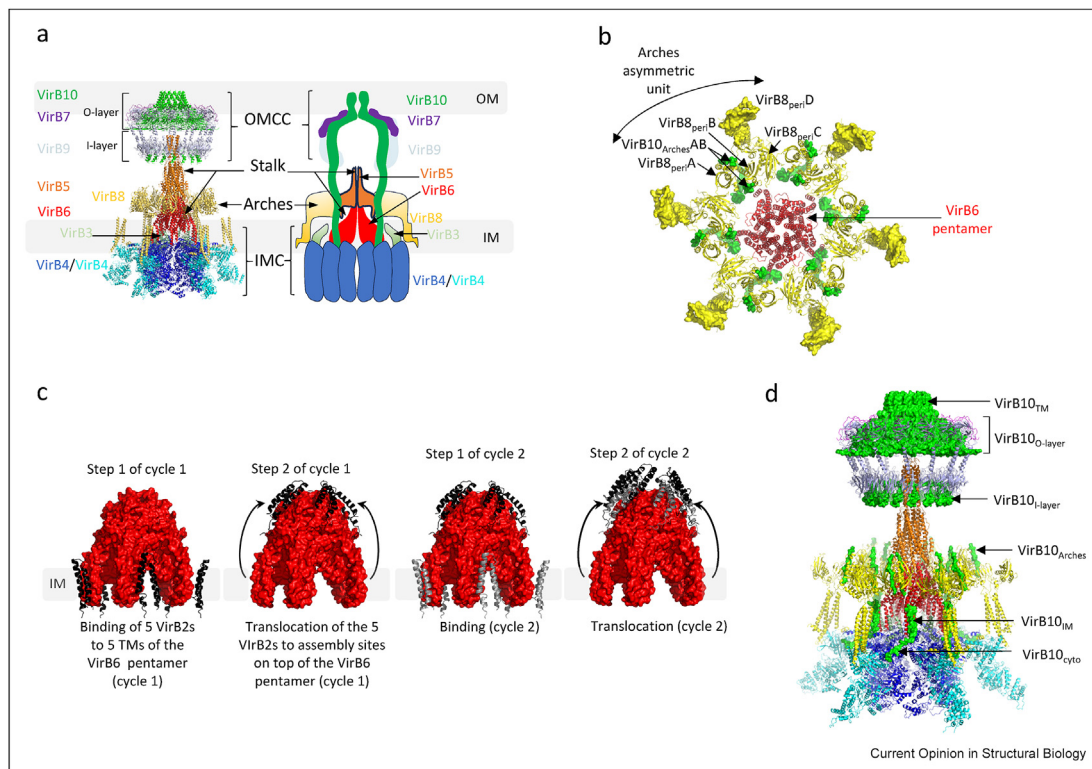
The type IV secretion system

Gram-negative T4SSs have been classified into two categories [22]: the minimized T4SS which contains 12 components, termed VirB1-11 and VirD4 (according to naming convention), and the expanded T4SS that contains additional subunits (although not always VirB11). Conjugative T4SSs belong to both categories.

In all Gram-negative bacterial conjugation systems, the T4SS is composed of four subcomplexes: the outer-membrane core complex (OMCC) embedded in the outer membrane, the inner membrane complex (IMC) in the inner membrane and two complexes primarily located in the periplasm, a stalk/cylinder bridging IMC and OMCC, and the arches/collar, surrounding the stalk base (Figure 2a) [23–25]. In minimized conjugative systems,

which are better known, the OMC is formed of 16 copies of the VirB7, VirB9, and VirB10. It is divided into two layers, the I-layer made of 16 of the N-terminal domains (NTD) of VirB9 and VirB10, and the O-layer is made of only 14 of the CTDs of VirB9 and VirB10 and also full-length VirB7 [25,26]. Recently, the O- and I-layer have been shown to exhibit great flexibility relative to one another [26]. The functional significance of the OMC layers symmetry mismatch and interlayer flexibility is unclear. The stalk is formed of two proteins: a pentamer of VirB5 sitting on top of a pentamer of VirB6, itself anchored into the IM via TM-helices. The arches around the base of the stalk are formed of 24 copies of the periplasmic domain of VirB8, 18 of which form a ring, while 6 of them protrude out (Figure 2b). Finally, the IMC is made of a hexamer of a newly defined extended

Figure 2



Cryo-EM structure of the R388 T4SS, role of the bitopic protein VirB10 and mechanism of pilus biogenesis by conjugative T4SS. **a**) Structure (left) and schematic diagram (right) of the T4SS from the R388 plasmid. At left, the structure as in Macé et al. (2022) [25] is shown in a ribbon diagram. All subunits are named the same color as in the structure and the diagram, except for the cyan and dark blue VirB4 subunits, which are all shown in dark blue in the diagram. **b**) New features of the most recent R388 T4SS [26] include 1- a fourth VirB8 subunit in the asymmetric unit of the arches, located at the periphery of the VirB8 periplasmic domain ring and 2- two VirB10 regions, VirB10_{Arches}, bound to two of the 4 VirB8 periplasmic domains in the asymmetric unit of the arches. Here, a top view of the arches (in surface representation) is shown with the VirB6 pentamer (part of the Stalk) in red ribbon. The curved double arrow indicates the extent of the asymmetric unit. It contains 4 periplasmic domains of VirB8, labeled VirB8_{peri}A-D, and two VirB10_{Arches} regions labeled VirB10_{Arches} A-B. **c**) Pilus biogenesis by conjugative T4SS. Two cycles of subunit incorporation alternating binding and translocation are shown. VirB6 (shown in red surface) acts as the platform onto which VirB2 pilus subunits (shown in black (cycle 1) and gray (cycle 2) ribbon) are recruited at TM sites in the membrane and then translocated to their assembly site located at the membrane-distal side of the VirB6 pentamer. At each cycle, a layer of 5 VirB2 subunits insert under the previously assembled layer. The ATPases responsible for translocation are unknown but are likely to be VirB4 and VirB11, located just under VirB6. **d**) The most recent R388 T4SS structure describes the most complete tracing of the protein VirB10, which extends from the OM channel to the cytoplasm. VirB proteins are as in panel a, except for VirB10, which is shown in surface representation. Of note is the interaction of the VirB10_{IM} segment that interacts with VirB6 at a site previously shown to be a site of VirB2 subunit binding. Thus, in this position, VirB10 inhibits pilus biogenesis. In the presence of the recipient cell, this inhibition is lifted, presumably because VirB10_{IM} dissociates from VirB6, allowing recruitment of VirB2 subunits and therefore pilus biogenesis to proceed.

protomer that was described recently as containing two VirB4s, one VirB3, four TM helices of VirB8 N-terminal tails, and the TM and cytoplasmic regions of VirB10 N-terminal tails [26]. Variations in IMC architectures have been noted: centrally located hexamers of protomers as described by cryo-electron tomography and high-resolution cryo-EM [23,25,26], and side-by-side protomeric hexamers as seen by negative-strain electron microscopy and also as suggested by the hexameric structure of VirB4 alone where hexamerization was stabilized by fusion to the constitutively-hexameric module hemolysin-coregulated protein (HCP) [24,25].

The T4SS high-resolution structure provided a plausible mechanism for pilus biogenesis [25]: central to this mechanism is the suggestion that the TMs of the VirB6 pentamer serve as a recruitment site for pilus subunits (VirB2) and that the periplasmic part of VirB6 serves as the assembly site for the pilus (Figure 2c). Thus, in each cycle of pilus subunit incorporation, five VirB2 subunits are recruited to their recruitment sites. They are next translocated to their assembly site on top of VirB6 by the synergized action of the VirB4 and VirB11 ATPases located underneath, freeing up the recruitment sites for 5 more VirB2s to bind. In the next cycle of translocation, the newly recruited VirB2s translocate to the assembly site to insert themselves under the first VirB2 pentameric layer. Cycle after cycle of subunit recruitment and translocation leads to a growing pilus that progressively extends through the arches, and then through the I- and O-layers and, finally, outside the cell, exposing the VirB5 subunit at its tip.

In their higher resolution work, Macé and Waksman provided details of VirB10, redefining some of its structural details (Figure 2d) [25,26]. VirB10 is a bitopic protein with its N-terminus in the cytoplasm and its C-terminus in the OMCC [27]. In fact, it contains only one folded domain, its CTD, the rest forming extended peptidic structures that interact with most components of the T4SS (Figure 2d): first a C-terminal soluble part in the cytoplasm (VirB10_{cyto}) that interacts with the IMC and its ATPase center, then an IM TM helix (VirB10_{IM}) that interacts with VirB6 TMs, followed by periplasmic segments that successively interact with the periplasmic domains of VirB8s in the arches (VirB10_{Arches}; Figure 2, b and d) and with the VirB9 NTD in the OMC I-layer (VirB10_{I-layer}), and finally a CTD that interacts with VirB9 CTD in the O-layer (VirB10_{O-layer}). There, VirB10 forms the outer membrane channel (VirB10_{OM}). Thus, VirB10 is ideally located to sense any extracellular signal (such as one emanating from contact with a recipient cell) and transmit it to the IMC ATPase center [27].

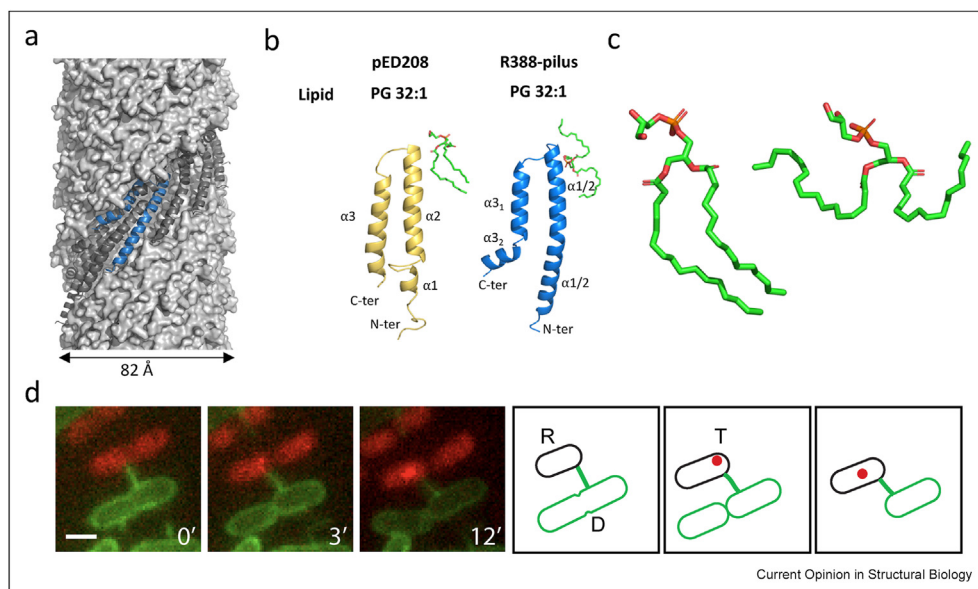
The pilus

Four conjugative pilus structures have been published in the last two years, one elaborated by the pKM101

plasmid [28], two structures of a pilus elaborated by the Ti plasmid [28,29] and one elaborated by the R388 plasmid [30]. They are essentially very similar to the first structure ever determined of a conjugative pilus, that elaborated by the F plasmid [31], consisting of a 5-array helical polymer of similar pitch and rise (Figure 3a). More importantly, they are all made of a polymerizing unit composed of a stoichiometric complex of a protein subunit, VirB2, and a phospholipid (Figure 3b). There are, however, variations on this theme. For example, the nature of the phospholipid may vary (see details in review by Costa et al., 2023 [6]). Recently, the publication of the pilus structure from the R388 plasmid provided distinct variations with apparently important biological consequences [30]. First, as opposed to all other pilus systems studied so far, this pilus was shown to be produced only when recipient cells are present, indicating that without recipient cells, pilus biogenesis in the donor cell is tightly inhibited. This observation was consistent with the fact that in the higher resolution structure of the corresponding T4SS by Macé and Waksman [26], VirB10_{IM} is shown to bind the VirB6 TM where VirB2 is recruited, thereby preventing VirB2 recruitment to VirB6 and thus inhibiting pilus biogenesis. It was hypothesized that the presence of recipient cells and the resulting contacts between cells may induce dissociation of VirB10_{IM} from VirB6 TMs, lifting the inhibitory effect of VirB10_{IM} on pilus biogenesis, and therefore leading to pilus formation. A second feature of the R388 pilus structure is that the two acyl chains of the phospholipid are splayed [30] (Figure 3b,c). In F or pED208 and other pilus systems, the chains are parallelly arranged [31] (Figure 3b,c). Interestingly, F and pED208 pili are known to be retractable, the phospholipid reintegrating its pool in the inner membrane, while doing so at no energy cost since the acyl chains are also parallel in the membrane. For R388, reintegration of the phospholipid in the membrane during retraction could be energetically costly, necessitating the acyl chains to transition from splayed to parallel. So it was hypothesized that the R388 pilus is unable to retract, and this was investigated experimentally by live cell imaging of the R388 pilus during conjugation. And indeed, no retraction event was observed [30].

Whether the pilus is the conduit for the relaxase-ssDNA conjugate has been the subject of debates. However, two reports have provided additional evidence that it is indeed the case. Using live cell imaging and adequate fluorescent probes, Goldlust et al. (2023) [32] and Beltrán et al. (2023) [33] were able to show that, although most cells undergo conjugation when in direct contact with each other, some are able to transfer DNA through the pilus (Figure 3d). However, the pilus may also operate (and, as a matter of fact, may be the sole operator) as a conduit for ssDNA even when cells are in direct contact: indeed, in conjugation systems like F-

Figure 3



Pilus structure and function. **a)** Structure of the R388 pilus. Four helical arrays are shown in gray surface, whereas one helical array is shown in gray ribbon except for one subunit in this array that is shown in blue as in panel b, right panel. The lipid is omitted from this representation. **b)** Structure of the VirB2 subunit of the F (left) and R388 (right) pilus. The type of lipid is indicated for each pilus. The structures are similar in that they both show bound structures with lipids, and are hairpin of helical elements. However, they differ slightly in the organization of these helical elements as detailed in Vadekkepat et al. (2024) [30]. Labeling of secondary structures is as in Ref. [30]. **c)** Zoom in on the lipid structure. Left: PG 32:1 observed in the F pilus; Right: PG 32:1 observed in the R388 pilus. Both are shown in such a way that the headgroups are in the same orientation. This view illustrates the fact that the two acyl chains in F are parallel while in R388, they are splayed. **d)** Plasmid transfer between physically distant cells. In this experiment conducted by Goldlust et al. (2023) [32], donor cell pilus subunits are labeled fluorescently green, while recipient cells express ParB fused to m-Cherry. Thus, the green fluorescence tracks the pilus while red fluorescence tracks dsDNA production. The first 3 panels at left show the data recorded at the indicated times after mixing donor and recipient cells. The last 3 panels at right report on a schematic interpretation of what is seen in each of the 3 left panels, respectively. From these results, it can be seen that cells may exchange DNA when distant from each other, provided that a pilus serves as a conduit to transport DNA from one to the other. Scale bar is 1 μm .

family plasmid (and unlike R388; see above), the pilus is known to retract [34] as the donor and recipient cells are brought into proximity, possibly leaving a mini-pilus to serve as substrate conduit through the membranes of the donor cell. However, this remains to be demonstrated.

Concerning the role of the phospholipid in pilus function, there's been speculation that without it, the lumen of the pilus would be lined with positive charges, hampering the transit of the ssDNA through the pilus. Recently, Patkowski et al. (2023) have established that the presence of phospholipids in the F pilus contributes to its structural stability, important for successful delivery of DNA during conjugation [35].

Mechanism of conjugation

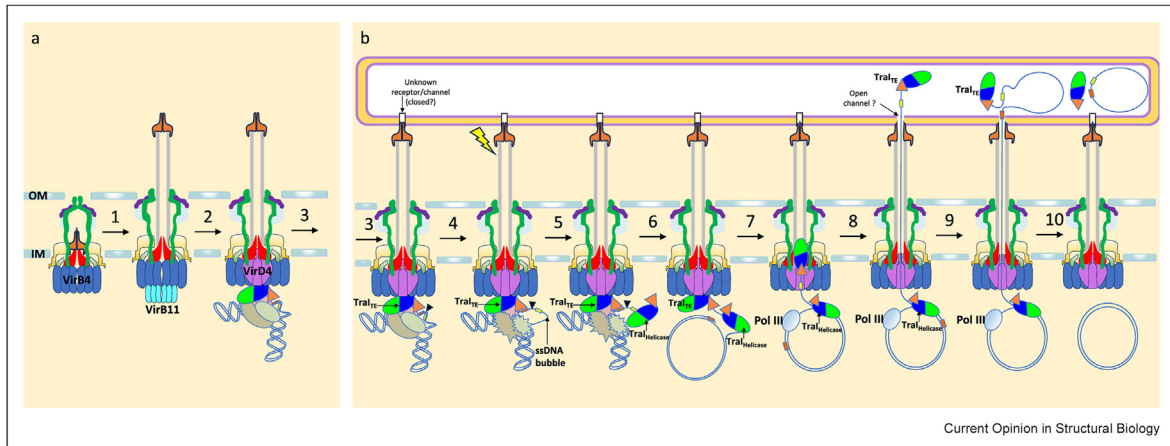
As progress is made in describing the succession of molecular events occurring during conjugation, a better grasp of its mechanism emerges, although many of the mechanistic details remain unknown.

A plausible mechanism for conjugation is described here (Figure 4). Conjugation starts with pilus biogenesis

powered by the combined action of the VirB4 and VirB11 ATPases (step 1 in Figure 4a; details in Figure 2c). Once pilus biogenesis is completed, VirB11 might dissociate, and the VirD4 ATPase (also referred to as coupling protein) is recruited to the T4SS (through its binding to VirB10_{cyto} [36]), simultaneously allowing recruitment of the relaxosome to the T4SS, which in the F plasmid system may occur via its interactions between VirD4 and TraM [20] and also interactions involving TraI [21] (step 2 in Figure 4a). The next steps in the conjugation process, those leading to substrate transfer to the recipient cell, are described in Figure 4b.

In F-family plasmids, the pilus is known to retract, and most conjugation events occur when donor and recipient cell membranes are in direct contact. The molecular basis for one such contact has been particularly well described recently, the interaction of TraN in the donor cell with Omp proteins in the recipient cell [37,38]. In the *Klebsiella pneumoniae* plasmid pKpQIL, TraN interacts with OmpK36, while TraN from the *Shigella flexneri* plasmid R100-1 or *Salmonella typhimurium* pSTL, interacts with OmpW and *Escherichia coli* F plasmid TraN

Figure 4



Conjugation mechanism. **a)** Pilus biogenesis. Pilus formation is shown in step 1 but the mechanism involves a number of steps illustrated in Figure 2c. In step 2, pilus biogenesis is completed and VirD4 replaces VirB11, in a still-unknown position (shown here centrally), and recruits the relaxosome. Here the F plasmid relaxosome is shown schematically as in Figure 1a. Relaxosomes always include a relaxase and IHF $\alpha\beta$, but the number of plasmid-encoded accessory proteins varies from 2 in F (TraY and TraM) to 1 in R388 (TrwA). **b)** The relaxase-ssDNA conjugated substrate transfer. The pilus makes contact with a recipient cell (perhaps through the interaction of the pilus tip protein VirB5 [43] and an unknown receptor ((indicated); step 3) and/or the donor and recipient cells are brought together by a retracting pilus to form tight junctions stabilized by the interaction between mating pair stabilization proteins (see main text). Establishment of these donor-recipient cell interactions activates a yet-to-be-identified signal (indicated by a bolt) that triggers the formation of a DNA bubble near the *nic* site (step 4), allowing a second Tral molecule to bind in its “closed” helicase conformation to the *tral*_{Helicase} binding site 3' of *nic* (step 5). This Tral will be used for DNA unwinding in the 5' to 3' direction. In the meantime, the relaxosome's Tral, presumably in its Tral_{TE} “open” conformation, binds to the *tral*_{TE} binding site 5' of *nic*, nicks the T-strand at *nic*, and covalently reacts to the 5' phosphate arising from the nicking reaction (step 6). This triggers the engagement and passage of the resulting relaxase-ssDNA conjugate through the T4SS and the pilus, and into the recipient cell (step 7). This requires the unfolding of the relaxase [44] and the unwinding of the dsDNA. The unfoldase is unknown; the helicase is Tral_{Helicase}. In this mechanism, unfolded Tral_{TE} is assumed to go first and then the ssDNA, although this remains to be demonstrated. Passage of the relaxase-ssDNA conjugate might require the opening of the VirB6 channel. Next, Tral_{TE}, once in the recipient cell, refolds, while the ssDNA is continually pushed through into the recipient cell through action of Tral_{Helicase} or the combined action of the VirD4 ATPase and Tral_{Helicase} (step 8). Once the end of the T-strand appears in the recipient cell (step 9), rejoining of the two ssDNA ends can occur in a reverse reaction to nicking and the plasmid is circularized (step 10). At this stage its replication in the recipient cell can occur. As does that of the R-strand (the one complementary to the T-strand) in the donor cell.

interacts with OmpA. Structural studies of TraN/Omp interactions and subsequent sequence analysis have identified several isoforms of TraN, revealing for the first time a potential mechanism for conjugative species specificity.

Many aspects of the mechanism presented in Figure 4 remain to be clarified or substantiated. For step 1, the mechanism of pilus biogenesis proposed by Macé et al. (2022) [25] requires further probing and the lever arm responsible for translocating VirB2 subunits from their VirB6 TM-binding site, out of the IM and on to their assembly sites remains to be identified. In step 2, it is not known where VirD4 locates within the conjugative T4SSs. Is it centrally placed as the negative-stained EM of the T4SS with VirD4 bound suggests [39]? Also unknown in steps 3 and 4 is the nature of the interaction partners that mediate the attachment of the pilus to the recipient cell surface, and that of the signal that arises from cell-cell or pilus-cell contacts and their mechanism of propagation to the IMC and relaxosome to create a DNA bubble around *nic*. Also unclear is the mechanism of engagement of the relaxase-ssDNA conjugated

substrate with and through the T4SS in step 7, as is the path of the substrate through the machinery and the identity of unfoldase that unfolds the relaxase. The possibility that the ATPase VirD4 in synergy with Tral_{Helicase} may drive the relaxase-ssDNA conjugate through the T4SS and the pilus remains to be tested. Interestingly, a recent report has described the inherent ability of relaxase-ssDNA conjugates to move through hemolysin nanopores at various speeds [40]. Also, in another report, Ryan et al. (2024) describes a potential implication of architectural asymmetry in enabling DNA transport [41]. Generally, the role of the striking symmetry mismatch we observed along the T4SS (16 and 14-fold symmetry of the I and O layers of the OMCC, the 5-fold symmetry of the stalk and the 6-fold symmetry of the IMC) remains to be clarified. Finally, how the 5'- and 3'-ends of the T-strand come within sufficient proximity for the relaxase to catalyze the reverse joining reaction and recircularize the plasmid DNA in the recipient cell is unknown. It also should be noted that the pilus biogenesis mechanism proposed by Macé et al. (2022) [25] might not apply to expanded conjugative T4SS, such as F-family plasmids. That's

because i- F-family systems have many more component subunits; ii- F-family systems have no VirB11; and iii- their VirB6 is much larger.

In conclusion, although initiated more than 70 years ago, the field of conjugation is in ebullition, energized by a number of new studies that have provided a plethora of new mechanistic insights. Such rapid progress raises the possibility that conjugation systems may be successfully targeted for inhibition to assist in the fight against the spread of antibiotic resistance. Given the demonstrated conserved and plastic features of T4SSs [42], one could safely assume that such compounds may work across many conjugative systems.

Declaration of competing interest

The authors declare that they have no known competing financial interests or personal relationships that could have appeared to influence the work reported in this paper.

Acknowledgements

This work was funded by Wellcome grant 217089 and MRC grant 01827 to GW. We thank Dr. Lesterlin for contribution of Figure 3c.

Data availability

No data was used for the research described in the article.

References

Papers of particular interest, published within the period of review, have been highlighted as:

- * of special interest
- ** of outstanding interest

1. Lederberg J, Tatum EL: **Gene recombination in *Escherichia coli***. *Nature* 1946, **158**:558.
2. Virolle C, Goldlust K, Djermoun S, Bigot S, Lesterlin C: **Plasmid transfer by conjugation in gram-negative bacteria: from the cellular to the community level**. *Genes* 2020, **11**:1239.
3. Barlow M: **What antimicrobial resistance has taught us about horizontal gene transfer**. *Methods Mol Biol* 2009, **532**:397–411.
4. **Antimicrobial Resistance Collaborators: global burden of bacterial antimicrobial resistance in 2019: a systematic analysis**. *Lancet* 2022, **399**:629–655.
5. Sheedlo MJ, Ohi MD, Lacy DB, Cover TL: **Molecular architecture of bacterial type IV secretion systems**. *PLoS Pathog* 2022, **18**, e1010720.
6. Costa TRD, Patkowski JB, Mace K, Christie PJ, Waksman G: **Structural and functional diversity of type IV secretion systems**. *Nat Rev Microbiol* 2023, **22**:170–185.
7. Zehra M, Heo J, Chung JM, Durie CL: **Comparative analysis of T4SS molecular architectures**. *J Microbiol Biotechnol* 2023, **33**:1543–1551.
8. Ryan ME, Damke PP, Shaffer CL: **DNA transport through the dynamic type IV secretion system**. *Infect Immun* 2023, **91**, e0043622.
9. Guzman-Herrador DL, Fernandez-Gomez A, Llosa M: **Recruitment of heterologous substrates by bacterial secretion systems for transkingdom translocation**. *Front Cell Infect Microbiol* 2023, **13**, 1146000.
10. Waksman G: **From conjugation to T4S systems in Gram-negative bacteria: a mechanistic biology perspective**. *EMBO Rep* 2019, **20**.
11. Zechner EL, Moncalian G, de la Cruz F: **Relaxases and plasmid transfer in gram-negative bacteria**. *Curr Top Microbiol Immunol* 2017, **413**:93–113.
12. Matson SW, Ragonese H: **The F-plasmid *Tral* protein contains three functional domains required for conjugative DNA strand transfer**. *J Bacteriol* 2005, **187**:697–706.
13. Luo Y, Gao Q, Deonier RC: **Mutational and physical analysis of F plasmid *traY* protein binding to *oriT***. *Mol Microbiol* 1994, **11**:459–469.
14. Rice PA, Yang S, Mizuuchi K, Nash HA: **Crystal structure of an IHF-DNA complex: a protein-induced DNA U-turn**. *Cell* 1996, **87**:1295–1306.
15. Ragonese H, Haisch D, Villareal E, Choi JH, Matson SW: **The F plasmid-encoded *TraM* protein stimulates relaxosome-mediated cleavage at *oriT* through an interaction with *Tral***. *Mol Microbiol* 2007, **63**:1173–1184.
16. Ilangovan A, Kay CWM, Roier S, El Mkami H, Salvadori E, Zechner EL, Zanetti G, Waksman G: **Cryo-EM structure of a relaxase reveals the molecular basis of DNA unwinding during bacterial conjugation**. *Cell* 2017, **169**:708–721.
17. Wong JJ, Lu J, Glover JN: **Relaxosome function and conjugation regulation in F-like plasmids - a structural biology perspective**. *Mol Microbiol* 2012, **85**:602–617.
18. Howard MT, Nelson WC, Matson SW: **Stepwise assembly of a relaxosome at the F plasmid origin of transfer**. *J Biol Chem* 1995, **270**:28381–28386.
19. Zechner EL, Lang S, Schildbach JF: **Assembly and mechanisms of bacterial type IV secretion machines**. *Philos Trans R Soc Lond B Biol Sci* 2012, **367**:1073–1087.
20. Lu J, Wong JJ, Edwards RA, Manchak J, Frost LS, Glover JN: **Structural basis of specific *TraD-TraM* recognition during F plasmid-mediated bacterial conjugation**. *Mol Microbiol* 2008, **70**:89–99.
21. Redzej A, Ilangovan A, Lang S, Gruber CJ, Topf M, Zangger K, Zechner EL, Waksman G: **Structure of a translocation signal domain mediating conjugative transfer by type IV secretion systems**. *Mol Microbiol* 2013, **89**:324–333.
22. Costa TRD, Harb L, Khara P, Zeng L, Hu B, Christie PJ: **Type IV secretion systems: advances in structure, function, and activation**. *Mol Microbiol* 2020, **115**:436–452.
23. Hu B, Khara P, Christie PJ: **Structural bases for F plasmid conjugation and F pilus biogenesis in *Escherichia coli***. *Proc Natl Acad Sci USA* 2019, **116**:14222–14227. U S A.
24. Low HH, Gubellini F, Rivera-Calzada A, Braun N, Connery S, Dujeancourt A, Lu F, Redzej A, Fronzes R, Orlova EV, et al.: **Structure of a type IV secretion system**. *Nature* 2014, **508**:550–553.
25. Macé K, Vadakkepat AK, Redzej A, Lukoyanova N, Oomen C, Braun N, Ukleja M, Lu F, Costa TRD, Orlova EV, et al.: **Cryo-EM structure of a type IV secretion system**. *Nature* 2022, **607**:191–196.
26. Mace K, Waksman G: **Cryo-EM structure of a conjugative type IV secretion system suggests a molecular switch regulating pilus biogenesis**. *EMBO J* 2024, **43**:3287–3306.
27. Cascales E, Christie PJ: ***Agrobacterium* VirB10, an ATP energy sensor required for type IV secretion**. *Proc Natl Acad Sci USA* 2004, **101**:17228–17233. U S A.

28. Amro J, Black C, Jemouai Z, Rooney N, Daneault C, Zeytuni N, Ruiz M, Bui KH, Baron C: **Cryo-EM structure of the *Agrobacterium tumefaciens* T-pilus reveals the importance of positive charges in the lumen.** *Structure* 2023, **31**:375–384.
29. Kreida S, Narita A, Johnson MD, Tocheva E, Das A, Ghosal D, Jenssen GJ: **Cryo-EM structure of the *Agrobacterium tumefaciens* T4SS-associated T-pilus reveals stoichiometric protein-phospholipid assembly.** *Structure* 2023, **31**:385–394.
30. Vadakkepat AK, Xue S, Redzej A, Smith TK, Ho BT, Waksman G: **Cryo-EM structure of the R388 plasmid conjugative pilus reveals a helical polymer characterized by an unusual pilin/phospholipid binary complex.** *Structure* 2024, **9**:1335–1347.
31. Costa TRD, Ilangovan A, Ukleja M, Redzej A, Santini JM, Smith TK, Egelman EH, Waksman G: **Structure of the bacterial sex F pilus reveals an assembly of a stoichiometric protein-phospholipid complex.** *Cell* 2016, **166**:1436–1444.
32. Goldlust K, Ducret A, Halte M, Dedieu-Berne A, Erhardt M, Lesterlin C: **The F pilus serves as a conduit for the DNA during conjugation between physically distant bacteria.** *Proc Natl Acad Sci U S A* 2023, **120**, e2310842120.
- In this publication, the authors provide convincing evidence that, while ssDNA transfer occur most often when cell are in contact, it may also occur between cells that are at some considerable distance from each other. In that case, transfer occurs through a pilus.
33. Beltrán L, Toorsilieri H, Patkowski JB, Yang JE, Casanova J, Costa TRD, Wright ER, Egelman EH: **The mating pilus of *E. coli* pED208 acts as a conduit for ssDNA during horizontal gene transfer.** *mBio* 2024, **15**, e0285723.
- In this study, the authors confirm that the pilus may act as conduit for ssDNA during conjugation.
34. Clarke M, Maddera L, Harris RL, Silverman PM: **F-pili dynamics by live-cell imaging.** *Proc Natl Acad Sci USA* 2008, **105**: 17978–17981. U S A.
35. Patkowski JB, Dahlberg T, Amin H, Gahlot DK, Vijayrajratnam S, Vogel JP, Francis MS, Baker JL, Andersson M, Costa TRD: **The F-pilus biomechanical adaptability accelerates conjugative dissemination of antimicrobial resistance and biofilm formation.** *Nat Commun* 2023, **14**:1879.
- This study shows that structural stability of the pilus conferred by the presence of PG32:1 is important for successful delivery of DNA during conjugation.
36. Llosa M, Zunzunegui S, De la Cruz F: **Conjugative coupling proteins interact with cognate and heterologous VirB10-like proteins while exhibiting specificity for cognate relaxosome.** *Proc Natl Acad Sci* 2003, **100**:10465–10470. USA.
37. Low WW, Wong JLC, Beltran L, Seddon C, David S, Kwong H-S, Bizeau T, Wang F, Pena A, Costa TRD, *et al.*: **Mating pair stabilization mediates bacterial conjugation species specificity.** *Nat Microbiol* 2022, **7**:1016–1027.
- The authors show that in F plasmids, the pairing between donor and recipient cells is stabilized by specific molecular interactions between TraN isoforms in the donor cell and Omp proteins in the recipient cell.
38. Low WW, Seddon C, Beis K, Frankel G: **The interaction of the F-like plasmid-encoded TraN isoforms with their cognate outer membrane receptors.** *J Bacteriol* 2023, **205**, e0006123.
39. Redzej A, Ukleja M, Connery S, Trokter M, Felisberto-Rodrigues C, Cryar A, Thalassinos K, Hayward RD, Orlova EV, Waksman G: **Structure of a VirD4 coupling protein bound to a VirB type IV secretion machinery.** *EMBO J* 2017, **36**: 3080–3095.
40. Valenzuela-Gomez F, Arechaga I, Cabezon E: **Nanopore sensing reveals a preferential pathway for the co-translocational unfolding of a conjugative relaxase-DNA complex.** *Nucleic Acids Res* 2023, **51**:6857–6869.
- Using hemolysin-based nanopore technology, the authors observe that cotranslocational unfolding of a conjugated relaxase-ssDNA substrate occurs in 7 steps. This constitutes the first attempt at characterizing the passage of the conjugated substrate through a pore.
41. Ryan ME, Damke PP, Bryant C, Sheedlo MJ, Shaffer CL: **Architectural asymmetry enables DNA transport through the *Helicobacter pylori* cag type IV secretion system.** *bioRxiv* 2023, <https://doi.org/10.1101/2023.07.25.550604>.
- The authors here suggest that architectural asymmetry orchestrates dynamic substrate selection and enables trans-kingdom DNA conjugation through the *Helicobacter pylori* cag type IV secretion system.
42. Kishida K, Li YG, Ogawa-Kishida N, Khara P, Al Mamun AAM, Bosserman RE, Christie PJ: **Chimeric systems composed of swapped Tra subunits between distantly-related F plasmids reveal striking plasticity among type IV secretion machines.** *PLoS Genet* 2024, **20**, e1011088.
- Comparing two F plasmid systems, the authors produce chimeras that reveal the extraordinary plasticity of T4SSs.
43. Aly KA, Baron C: **The VirB5 protein localizes to the T-pilus tips in *Agrobacterium tumefaciens*.** *Microbiology* 2007, **153**: 3766–3775.
44. Trokter M, Waksman G: **Translocation through the conjugative type IV secretion system requires unfolding of its protein substrate.** *J Bacteriol* 2018, **23**, e00615-17.